

# Finite-nuclear-size effect for hydrogenlike ions under high external pressure

Dengshan Liu,<sup>1</sup> Huihui Xie,<sup>1</sup> Pengxiang Du,<sup>1</sup> Tianshuai Shang,<sup>1</sup>

Jian Li <sup>a,1,2</sup>, Jiguang Li,<sup>3</sup> and Tomoya Naito<sup>4,5,6</sup>

<sup>1</sup>*College of Physics, Jilin University, Changchun 130012, China*

<sup>2</sup>*Institute of Theoretical Physics, Chinese Academy of Sciences, Beijing 100190, China*

<sup>3</sup>*Institute of Applied Physics and Computational Mathematics, Beijing 100088, China*

<sup>4</sup>*Department of Nuclear Engineering and Management,  
Graduate School of Engineering, The University of Tokyo, Tokyo 113-8656, Japan*

<sup>5</sup>*Department of Physics, Graduate School of Science,  
The University of Tokyo, Tokyo 113-0033, Japan*

<sup>6</sup>*RIKEN Center for Interdisciplinary Theoretical and  
Mathematical Sciences (iTHEMS), Wako 351-0198, Japan*

## Abstract

The influence of pressure on finite-nuclear-size (FNS) corrections to atomic energy levels and electron-capture decay rate is investigated in confined hydrogenlike ions. The ions are modeled inside an impenetrable spherical cavity, with a Gaussian distribution used to represent the nuclear charge distribution. For each confinement radius—used to simulate external pressure—the energies and wave functions of the lowest-lying bound states are determined by numerically solving the Dirac equation via the kinetically balanced generalized pseudospectral (KBGPS) method. In contrast to unconfined ions, both the FNS corrections and electron-capture decay rates increase markedly under pressure and exhibit parallel trends with increasing confinement. Pressure also removes level degeneracies and alters the relative magnitudes of FNS corrections across different bound states. Moreover, the nuclear charge radius is found to significantly affect the pressure-enhanced electron-capture decay rate.

PACS numbers: 23.40.-s, 21.10.Ft, 31.15.-p

Keywords: finite-nuclear-size effects, hydrogen-like ions, electron capture decay, high external pressure

---

<sup>a</sup> Corresponding author:: jianli@jlu.edu.cn

## I. INTRODUCTION

In state-of-the-art electronic structure calculations of atoms and molecules [1, 2], it is essential to consider the finite-nuclear-size effect, which accounts for the fundamental discrepancy between the conventional point-nucleus approximation and the physical reality of spatially extended nuclear charge distributions. For highly charged ions with a large nuclear charge, corrections due to the FNS effect on energy levels can be up to hundreds of electron volts [3–8]. Moreover, FNS effects on the weak decay processes of elementary particles involving electrons, i.e.,  $\beta$  decay [9, 10] and electron-capture decay [11, 12], have been considered for a long time.

Hydrogenlike ions possess the simplest electronic structure, making them ideal systems for theoretical studies of FNS effects, and the investigation of FNS effects in these systems holds critical implications for fundamental research [13–21]. For example, FNS corrections to the bound-electron energy levels and  $g$  factors of hydrogenlike ions could serve as critical benchmarks for stringent tests of quantum electrodynamics (QED) [17–21]. Additionally, accurate calculations of transition probabilities in hydrogenlike ions necessitate the inclusion of FNS corrections [22–24]. Until now, for free hydrogenlike ions, the study of the FNS effect has been very comprehensive. Studying the variation of these quantities for hydrogenlike ions under external pressure is of great significance.

In 1937, the confined hydrogen atom model [25] was proposed to study the variations in the polarizability and kinetic energy of a hydrogen atom subjected to high external pressure. This model assumes that the atomic nucleus is fixed at the center of an impenetrable spherical cavity, while the electron is constrained to move within this enclosed region. By varying the size of the enclosed region, the model can mimic the compression of the electron cloud under different external pressures. Since this system does not require consideration of a large number of hydrogenlike ions and only focuses on a single hydrogenlike ion, it has attracted widespread attention over the subsequent decades. Studies have extensively examined the energy levels [26–28], transition probabilities [29], and polarizability of confined hydrogen atoms and hydrogenlike ions [30–32]. In Ref. [33], the Schrödinger equation for the confined hydrogen atom was solved to investigate the dependence of finite-nuclear-size corrections on external pressure, which reveals that these corrections to the energy levels increase significantly with increasing external pressure. Given the notable impact of external pressure on FNS corrections to hydrogen atomic energy levels, together with the non-negligible relativistic effects in heavier hydrogenlike ions, it is imperative to utilize

the Dirac equation to explore the corresponding relativistic FNS effects in hydrogenlike ions under these extreme conditions.

Moreover, the interiors of stellar plasmas are subjected to extreme pressure, extreme conditions where hydrogenlike ions become highly abundant [34]. The decay properties of such ions differ significantly from those of neutral atoms [35–41], and understanding their decay modes is crucial for clarifying key processes in stellar nucleosynthesis. Experimental studies have been conducted on various hydrogenlike ions [40, 42, 43]; for instance,  $\beta^+$  and electron-capture decays have been investigated in the hydrogenlike ion  $^{140}\text{Pr}^{58+}$  [37]. Although radioactive decay is generally considered to be independent of the external environment, the electron-capture decay rate ( $\lambda_{\text{EC}}$ ) is an exception. It depends strongly on external conditions [44–51], since it is proportional to the electron density at the nucleus [11]. Therefore, it is crucial to study the influence of external pressure on electron-capture decay in hydrogenlike ions.

In this paper, the effects of pressure on FNS corrections to energy levels and the decay rate of electron-capture decay are systematically investigated by means of the confinement model. The paper is organized as follows. In Sect. II, the point-nucleus Coulomb potential and the Gaussian charge distribution model potential for confined hydrogenlike ions are introduced, along with the definition of the FNS correction for atomic energy levels under pressure. In Sect. III and Sect. IV, the FNS corrections to the energy levels and the decay rate of electron-capture decay for hydrogenlike ions under high pressure are systematically analyzed, respectively. Finally, conclusions and an outlook are presented in Sect. V.

## II. THEORETICAL METHOD

The effects of pressure on FNS corrections to energy levels and the decay rate of electron-capture decay are studied using the confinement model. The hydrogenlike ion under isotropic pressure is modeled by confining it within an impenetrable spherical box with confinement radius  $R_0$ . The corresponding point-nucleus Coulomb potential reads

$$V(r) = \begin{cases} -\frac{eZ}{r}, & r < R_0, \\ \infty, & r \geq R_0, \end{cases} \quad (2.1)$$

where  $Z$  is the atomic number. To consider the finite nuclear charge density distributions, the Gaussian charge distribution model [7] is used. It should be noted that although more accurate nuclear charge densities are available [52–54], a simple Gaussian charge density distribution model

featuring an analytical Coulomb potential is adopted to facilitate discussions and calculations here. The corresponding potential with impenetrable walls is expressed as

$$V(r) = \begin{cases} -\frac{eZ}{r}\text{erf}(\sqrt{\xi}r), & r < R_0, \\ \infty, & r \geq R_0 \end{cases} \quad (2.2)$$

with  $\xi = \frac{3}{2r_c^2}$ , where  $r_c$  is the root-mean-square nuclear charge radii and  $\text{erf}(x)$  is the error function. For the relativistic Dirac equation of the one-electron system, i.e., hydrogenlike ion, after separating out the angular parts of the wave function, the radial Dirac equation is given by:

$$\begin{pmatrix} V(r) & -c(\frac{d}{dr} - \frac{\kappa}{r}) \\ c(\frac{d}{dr} + \frac{\kappa}{r}) & V(r) - 2c^2 \end{pmatrix} \begin{pmatrix} P_{n\kappa}(r) \\ Q_{n\kappa}(r) \end{pmatrix} = E \begin{pmatrix} P_{n\kappa}(r) \\ Q_{n\kappa}(r) \end{pmatrix}. \quad (2.3)$$

Substituting the above potential fields, Eq. (2.1) or Eq. (2.2), into the radial Dirac equation (2.3) yields the energy eigenvalues  $E_{\text{Gauss}}[n\kappa]$  or  $E_{\text{point}}[n\kappa]$  [7], respectively, as well as the electron density at the nucleus,  $\rho(0)$ . The FNS correction to atomic energy levels under pressure is expressed as

$$\Delta E_{\text{FNS}} = E_{\text{Gauss}} - E_{\text{point}}. \quad (2.4)$$

Additionally, the hydrostatic pressure  $P$  exerted on the electronic system by confinement effects can be estimated based on the variation of the ground-state energy with changes in the confinement volume [28], i.e.,

$$P = -\frac{1}{4\pi R_0^2} \frac{dE}{dR_0}. \quad (2.5)$$

The electron-capture decay rate ( $\lambda_{\text{EC}}$ ) is proportional to the electron density at the nucleus, i.e.,  $\lambda_{\text{EC}} \propto \rho(0)$ , and the variation of  $\rho(0)$  depends on the confinement radius  $R_0$ . The relationship between the external pressure and the confinement radius can be described by Eq. (2.5), from which the relationship between the fractional increase of the decay rate [44, 45] and the external pressure can be derived [47]:

$$\frac{\lambda - \lambda_0}{\lambda_0} = \frac{\rho(0) - \rho(0)_{\text{ref}}}{\rho(0)_{\text{ref}}}, \quad (2.6)$$

where  $\lambda_0$  is the reference electron-capture decay rate at zero pressure,  $\rho(0)_{\text{ref}}$  is the corresponding electron density at the nucleus when there is no pressure, and  $\lambda$  is the decay rate under pressure. Both  $\rho(0)_{\text{ref}}$  and  $\rho(0)$  are derived from solving the Dirac equation; therefore, they inherently account for relativistic effects.

### III. PRESSURE EFFECTS ON FNS CORRECTIONS TO ENERGY LEVELS

Figure 1 (a) and (b) display the absolute energy values  $|E_{1s}|$  — which incorporates the FNS effect — and corresponding FNS correction to energy levels  $\Delta E_{\text{FNS}}$  for the ground state of hydrogenlike ions  ${}^7\text{Be}^{3+}$ ,  ${}^{56}\text{Fe}^{25+}$ ,  ${}^{120}\text{Sn}^{49+}$  and  ${}^{208}\text{Pb}^{81+}$ , respectively, as a function of pressure. The calculations cover a pressure range from 1 GPa to  $10^{17}$  GPa. Owing to the significant variations in both the  $|E_{1s}|$  and  $\Delta E_{\text{FNS}}$  across this pressure range, a logarithmic scale is used for the vertical axis in Fig. 1 to better represent their behavior, and the absolute values of the energy levels are plotted.

Figure 1(a) clearly illustrates that the ground-state energy  $E_{1s}$  increases monotonically with pressure. At low pressures, the energy levels approach those of free hydrogenlike ions asymptotically, remaining negative. As pressure increases, the energies rise gradually toward zero. With

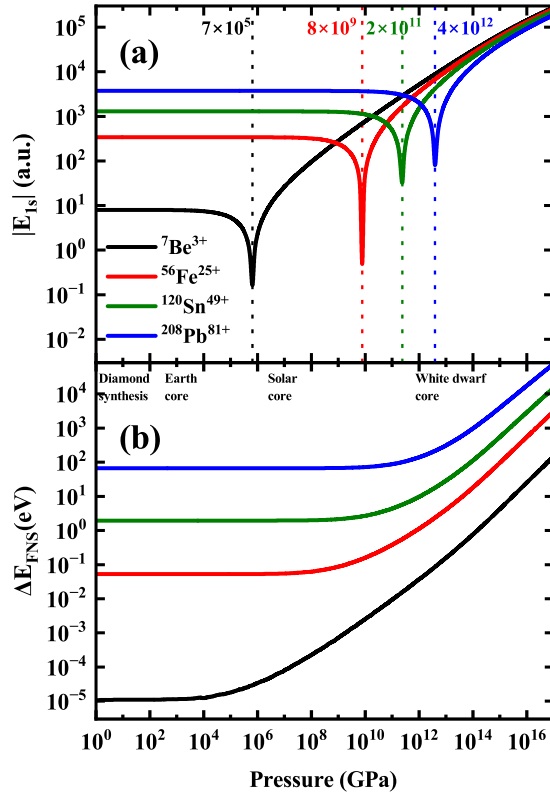


FIG. 1. The absolute energy values  $|E_{1s}|$  (a) and the corresponding FNS correction  $\Delta E_{\text{FNS}}$  (b) for the  $1s_{1/2}$  state of hydrogenlike ions  ${}^7\text{Be}^{3+}$ ,  ${}^{56}\text{Fe}^{25+}$ ,  ${}^{120}\text{Sn}^{49+}$  and  ${}^{208}\text{Pb}^{81+}$  as a function of pressure. The vertical dashed line of (a) represents the pressure where the energy level is zero. At the top of (b), some characteristic pressures are labeled that represent several orders of magnitude.

further increase in pressure, the energy values eventually exceed zero and exhibit a rapid increase. This behavior arises because higher pressure leads to greater localization of the corresponding wave function. According to the Heisenberg uncertainty principle, enhanced localization increases momentum. The pressure at which the energy level reaches zero is defined as the critical pressure, indicated by the dashed lines in Fig. 1(a). On both sides of this critical point, the energy levels display markedly different trends. A comparison of critical pressures among different hydrogenlike ions reveals that those with smaller nuclear charges have lower critical pressures. For instance, the critical pressure increases from  $7 \times 10^5$  GPa in  ${}^7\text{Be}^{3+}$  to  $8 \times 10^9$  GPa in  ${}^{56}\text{Fe}^{25+}$ ,  $2 \times 10^{11}$  GPa in  ${}^{120}\text{Sn}^{49+}$  and  $4 \times 10^{12}$  GPa in  ${}^{208}\text{Pb}^{81+}$ . This is because hydrogenlike ions with smaller nuclear charges possess ground state wavefunctions distributed over a larger spatial extent, rendering them more susceptible to compression under pressure and thus more sensitive to external confinement.

It can be observed from Fig. 1(b) that when the pressure is below the critical pressure,  $\Delta E_{\text{FNS}}$  increases very slowly. As the pressure approaches the critical pressure,  $\Delta E_{\text{FNS}}$  starts to increase rapidly and continues to grow with further pressure increases. This indicates that as the pressure increases, the FNS effect becomes progressively more significant. Although the ground state of hydrogenlike ions is bound by an infinite potential barrier rather than the Coulomb potential when the pressure exceeds the critical value, the strong external pressure compresses the electron wavefunction toward the nucleus, thereby enhancing the FNS effect. Lighter hydrogenlike ions are more sensitive to pressure; the magnitude of  $\Delta E_{\text{FNS}}$  in light hydrogenlike ions increases much faster than in heavy hydrogenlike ions. For example,  $\Delta E_{\text{FNS}}$  in  ${}^7\text{Be}^{3+}$  is about seven orders of magnitude smaller than in  ${}^{208}\text{Pb}^{81+}$  at approximately 100 GPa, and it finally becomes three orders of magnitude smaller as pressure approaches  $10^{16}$  GPa. In Fig. 1(b), the orders of magnitude of several characteristic pressures are presented to give an idea of the pressures involved.

It is meaningful to investigate the effect of pressure on different bound states. Fig. 2(a) and (b) present the absolute values of energy levels and corresponding FNS corrections  $\Delta E_{\text{FNS}}$  as a function of pressure for  $1s_{1/2}$ ,  $2s_{1/2}$  and  $2p_{1/2}$  states in hydrogenlike ion  ${}^{120}\text{Sn}^{49+}$ . It can be observed from Fig. 2 that the critical pressures of excited states of the hydrogenlike ion  ${}^{120}\text{Sn}^{49+}$  are lower than those of the ground state. This is attributed to the fact that the energy levels of the excited states are higher than those of the ground state, and with increasing pressure, the energy levels of the excited states converge toward zero more swiftly. Furthermore, the critical pressures of the  $2s_{1/2}$  and  $2p_{1/2}$  states are relatively close; when the pressure approaches their critical pressures, about  $10^6$  GPa, the difference between their energy levels becomes increasingly

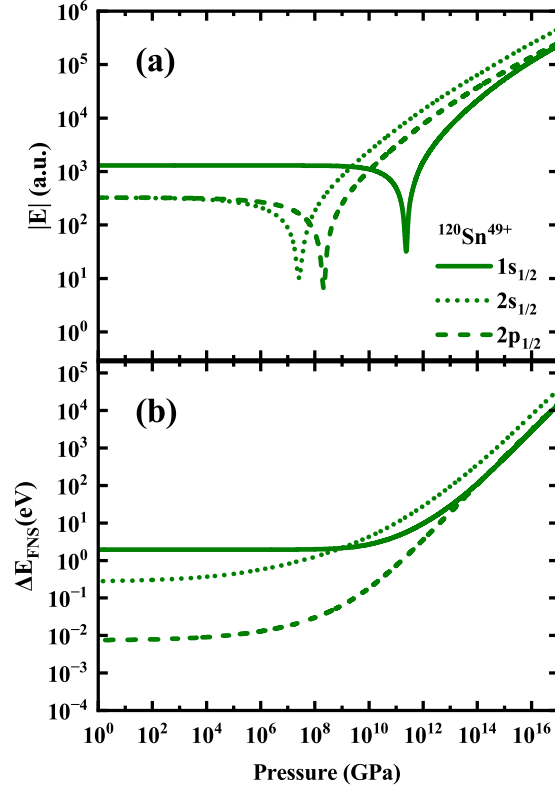


FIG. 2. Absolute values of energy levels (a) and FNS corrections to energy levels  $\Delta E_{\text{FNS}}$  (b) for  $1s_{1/2}$ ,  $2s_{1/2}$  and  $2p_{1/2}$  states of hydrogenlike ion  $^{120}\text{Sn}^{49+}$  as a function of pressure.

prominent. Subsequently, with further increases in pressure, the energy level of  $2s_{1/2}$  state remains higher than that of the  $2p_{1/2}$  state. However, once the pressure exceeds the critical pressure of the  $1s_{1/2}$  state, the energy level of  $1s_{1/2}$  state gradually approaches that of the  $2p_{1/2}$  state, driven by increasingly prominent relativistic effects under high-pressure conditions.

In Fig. 2(b), by comparing FNS corrections  $\Delta E_{\text{FNS}}$  for different bound states, it can be observed that at low pressure, the  $\Delta E_{\text{FNS}}$  for  $1s_{1/2}$  state is higher than that for  $2s_{1/2}$  state, and the  $\Delta E_{\text{FNS}}$  for  $2s_{1/2}$  state is higher than that for  $2p_{1/2}$  state. This is consistent with the statement in Ref. [7]. However, when the pressure reaches  $10^9$  GPa, the  $\Delta E_{\text{FNS}}$  in  $2s_{1/2}$  state exceeds that in the  $1s_{1/2}$  state, and as the pressure increases further, the difference in  $\Delta E_{\text{FNS}}$  between the two states continues to grow. Meanwhile,  $\Delta E_{\text{FNS}}$  in the  $2p_{1/2}$  state gradually approaches that in the  $1s_{1/2}$  state, and after the pressure exceeds  $10^{14}$  GPa,  $\Delta E_{\text{FNS}}$  of the two states become nearly equal. Therefore, from this figure, it can be seen that the relative magnitudes of  $\Delta E_{\text{FNS}}$  for different bound states undergo significant changes with increasing pressure.

In studies of confined atomic systems, the nonrelativistic Schrödinger equation is commonly

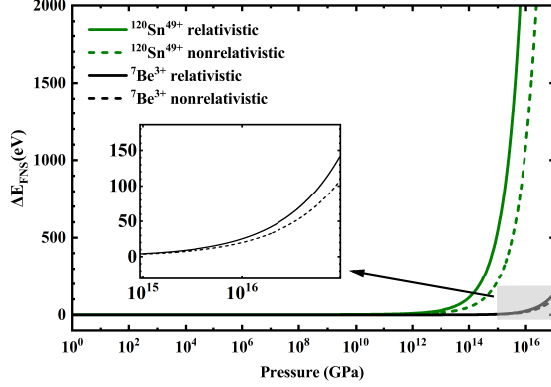


FIG. 3.  $\Delta E_{\text{FNS}}$  for the  $1s_{1/2}$  state of hydrogenlike ions  ${}^7\text{Be}^{3+}$  and  ${}^{120}\text{Sn}^{49+}$  in the relativistic case, are compared with the nonrelativistic case.

used. However, this formulation does not account for relativistic effects, which play a significant role in hydrogenlike ions with high nuclear charge or under high-pressure conditions. It is therefore essential to evaluate the influence of relativistic corrections on  $\Delta E_{\text{FNS}}$ . To address this, the nonrelativistic Schrödinger equation for confined hydrogen-like ions is solved considering both Gaussian and point-like nuclear charge distributions, yielding the corresponding nonrelativistic values of  $\Delta E_{\text{FNS}}$ . These results are subsequently compared with those derived from the Dirac equation. The numerical solution of the Schrödinger equation is obtained via the generalized pseudospectral (GPS) method. The GPS method is a discrete variable representation approach based on global basis functions and Gauss-type quadratures [55], which transforms the differential equation into a matrix eigenvalue problem by mapping the infinite domain onto a finite interval. Implemented within the discrete-variable representation framework, the GPS method demonstrates rapid convergence and high versatility in solving quantum eigenvalue problems [55–59]. Furthermore, significant progress has also been made in solving the Dirac and Schrödinger equations using machine learning [60, 61].

Figure 3 compares the FNS corrections to energy levels  $\Delta E_{\text{FNS}}$  for the  $1s_{1/2}$  state of hydrogenlike ions  ${}^7\text{Be}^{3+}$  and  ${}^{120}\text{Sn}^{49+}$  between the relativistic and nonrelativistic cases. The relativistic  $\Delta E_{\text{FNS}}$  is consistently greater than its nonrelativistic counterpart. Furthermore, the disparity in  $\Delta E_{\text{FNS}}$  attributable to relativistic effects intensifies significantly with increasing pressure. Beyond pressures of  $10^{14}$  GPa, this difference becomes particularly pronounced for the hydrogenlike ion  ${}^{120}\text{Sn}^{49+}$ . In contrast, for  ${}^7\text{Be}^{3+}$  within the same pressure range, the differences are considerably smaller than those observed for  ${}^{120}\text{Sn}^{49+}$ . Consequently, accounting for relativistic effects is

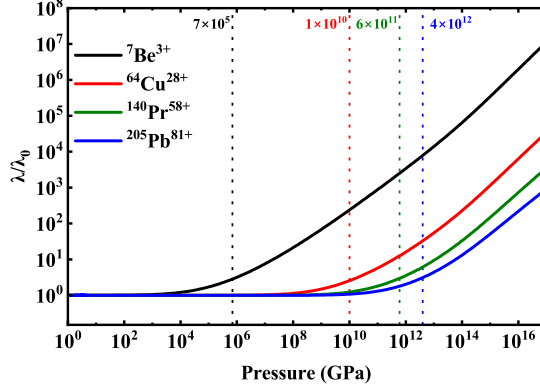


FIG. 4. The ratio of the electron-capture decay rate with and without pressure for the  $1s_{1/2}$  state of hydrogenlike ions  ${}^7\text{Be}^{3+}$ ,  ${}^{64}\text{Cu}^{28+}$ ,  ${}^{140}\text{Pr}^{58+}$  and  ${}^{205}\text{Pb}^{81+}$  as a function of pressure. The vertical dashed line denotes the critical pressure for the corresponding hydrogenlike ions.

essential for hydrogenlike ions with higher nuclear charges under extreme pressure conditions.

#### IV. THE EFFECT OF PRESSURE ON ELECTRON-CAPTURE DECAY

Figure 4 displays the ratio between the electron-capture decay rate of  ${}^7\text{Be}^{3+}$ ,  ${}^{64}\text{Cu}^{28+}$ ,  ${}^{140}\text{Pr}^{58+}$  and  ${}^{205}\text{Pb}^{81+}$  under pressure and that at zero pressure. By observing the relationship between the ratio and pressure, it is evident that the variation of the electron-capture decay rate under pressure exhibits a significant similarity to the changes in the FNS corrections to energy levels  $\Delta E_{\text{FNS}}$  under pressure. For example, when the pressure is below the critical pressure, there is no significant change in the electron-capture decay rate. However, as the pressure approaches the critical pressure, the electron-capture decay rate increases rapidly with the pressure. The ratio of the electron-capture decay rate for hydrogenlike ion  ${}^7\text{Be}^{3+}$  has increased by approximately seven orders of magnitude within the current pressure range. Moreover, as the pressure reaches to  $10^6$  GPa (approximately equal to the pressure at the solar core), the electron-capture decay rate of  ${}^7\text{Be}^{3+}$  ions has already undergone a significant change; thus, this is likely to exert an important influence on the hydrogen burning process inside the Sun. For nuclides with a larger proton number, a significant change in the electron-capture rate would only be possible at higher pressures.

As the electron density at the nucleus  $\rho(0)$  depends not only on external pressure but also critically on the nuclear charge radius, the latter plays a significant role in modulating  $\rho(0)$ . The

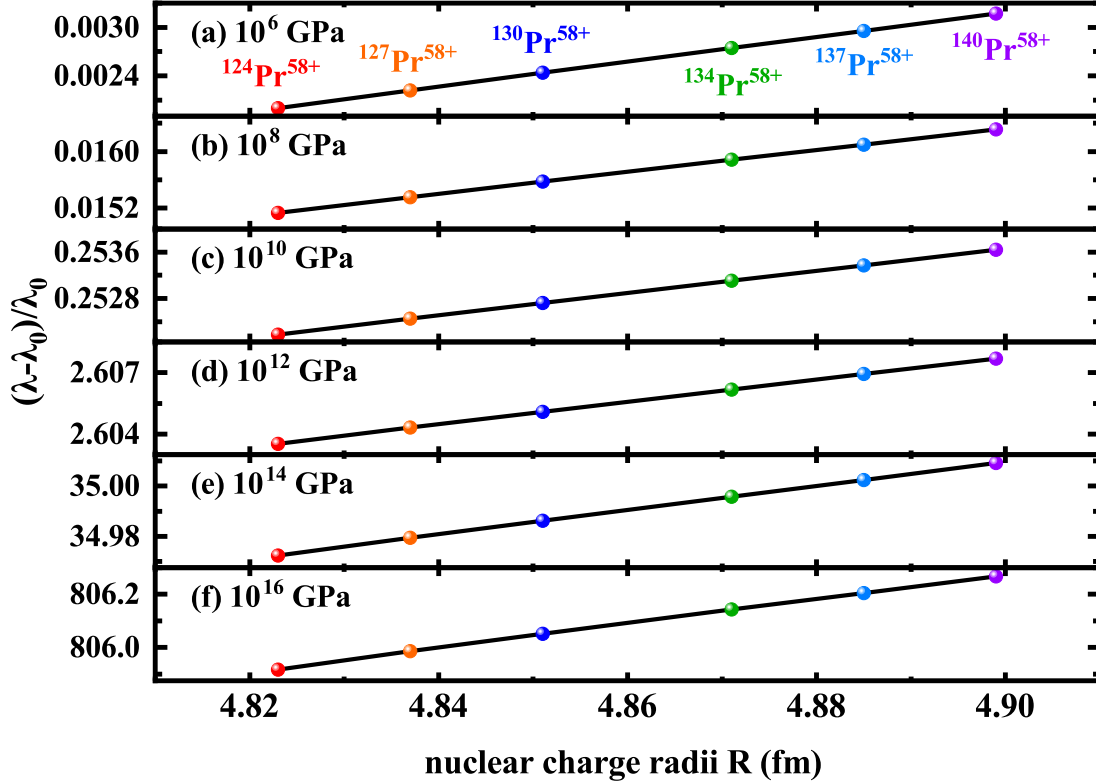


FIG. 5. The fractional increase of the decay rate at the  $1s_{1/2}$  state of hydrogenlike ions of Pr isotopes. (a) Fixed different pressures at  $10^6$  GPa, (b)  $10^8$  GPa, (c)  $10^{10}$  GPa, (d)  $10^{12}$  GPa, (e)  $10^{14}$  GPa, and (f)  $10^{16}$  GPa.

variation in nuclear charge radii across an isotope chain motivates a detailed investigation of the electron-capture decay rates among these nuclides under high external pressure. Figure 5 depicts  $(\lambda - \lambda_0)/\lambda_0$  for the  $1s_{1/2}$  state of hydrogenlike ions of Pr isotopes at several different pressure magnitudes. It can be observed that  $(\lambda - \lambda_0)/\lambda_0$  rises with the increase of nuclear charge radius. This indicates that pressure has a more significant effect on isotopes with larger nuclear charge radii.

In Fig. 5(a), the pressure is  $10^6$  GPa, which is roughly equivalent to the pressure at the core of the sun,  $(\lambda - \lambda_0)/\lambda_0$  increases from 0.002 to 0.003 as the nuclear charge radii  $r_c$  increases from 4.823 to 4.899 fm. This indicates that, within the current pressure range, the influence of the nuclear charge radius on the decay rate is roughly comparable to the effect of external pressure on that. However, as the pressure increases, the influence of pressure on the decay rate gradually becomes dominant.

## V. CONCLUSIONS AND DISCUSSIONS

In summary, the pressure dependence of FNS effects and electron-capture decay rates has been investigated for different hydrogenlike ions by using the confined atom model. It is found that both the FNS energy corrections  $\Delta E_{\text{FNS}}$  and the electron-capture decay rate increase monotonically as pressure increases. Based on the pressure-induced evolution of energy levels, a critical pressure was defined, which is shown to play a key role in governing the behavior of both FNS corrections and decay rates under compression. The magnitudes of FNS corrections to energy levels for  $1s_{1/2}$ ,  $2s_{1/2}$  and  $2p_{1/2}$  states change as pressure increases. Additionally, it is essential to consider the relativistic effects for the  $\Delta E_{\text{FNS}}$  under extreme pressure conditions. Investigation of Pr isotopes revealed that isotopes with larger nuclear charge radii exhibit a greater fractional increase in electron-capture decay rate under pressure.

Our results show that certain nuclear-related quantities undergo significant modifications under high pressure. Existing experimental studies have already demonstrated that confinement effects can alter the electron-capture decay rate of beryllium [48–51]. Therefore, future studies will extend this methodology by employing the confined atom model to investigate the effects of pressure on electron-capture decay in multi-electron systems. Furthermore, research on high-pressure single-atom systems holds promise as a prospective research direction in the field of high-pressure physics. Under high-pressure conditions, numerous atoms form solid phases, a subset of which are metallic [62]. Accounting for such phase transitions in the context of electron-capture decay rates is also essential, and this aspect is reserved for future investigations.

## ACKNOWLEDGMENTS

Dengshan Liu, Huihui Xie, Pengxiang Du, Tianshuai Shang and Jian Li acknowledge the National Natural Science Foundation of China (Grants No. 12475119 and 12447101) and the China Postdoctoral Science Foundation, No. 2025M783390. Tomoya Naito acknowledges the JSPS Grant-in-Aid under Grant Nos. JP23H01845, JP23K03426, JP23K26538, JP24K17057,

- [1] D. Andrae, Finite nuclear charge density distributions in electronic structure calculations for atoms and molecules, *Phys. Rep.* **336**, 413 (2000).
- [2] D. Andrae, in *Theoretical and Computational Chemistry*, Vol. 11 (Elsevier, 2002) p. 203.
- [3] V. M. Shabaev, Finite nuclear size corrections to the energy levels of the multicharged ions, *J. Phys. B: At. Mol. Opt. Phys.* **26**, 1103 (1993).
- [4] R. T. Deck, J. G. Amar, and G. Fralick, Nuclear size corrections to the energy levels of single-electron and -muon atoms, *J. Phys. B: At. Mol. Opt. Phys.* **38**, 2173 (2005).
- [5] B. N. Niri and A. Anjami, Nuclear size corrections to the energy levels of single-electron atoms, *Nucl. Sci.* **3**, 1 (2018).
- [6] I. A. Valuev, Z. Harman, C. H. Keitel, and N. S. Oreshkina, Skyrme-type nuclear interaction as a tool for calculating the finite-nuclear-size correction to atomic energy levels and the bound-electron g factor, *Phys. Rev. A* **101**, 062502 (2020).
- [7] H. H. Xie, J. Li, L. G. Jiao, and Y. K. Ho, Finite-nuclear-size effect in hydrogenlike ions with relativistic nuclear structure, *Phys. Rev. A* **107**, 042807 (2023).
- [8] I. Kuzmenko, T. Kuzmenko, Y. Avishai, and Y. B. Band, Hydrogen and hydrogenlike-ion bound states and hyperfine splittings: Finite-nuclear-size effects, *Phys. Rev. A* **108**, 052804 (2023).
- [9] O. Nițescu, S. Ghinescu, and S. Stoica, Lorentz violation effects in  $2\nu\beta\beta$  decay, *J. Phys. G: Nucl. Part. Phys.* **47**, 055112 (2020).
- [10] O. Nițescu, R. Dvornický, and F. Šimkovic, Atomic corrections for the unique first-forbidden  $\beta$  transition of  $^{187}\text{Re}$ , *Phys. Rev. C* **109**, 025501 (2024).
- [11] W. Bambynek, H. Behrens, M. H. Chen, B. Crasemann, M. L. Fitzpatrick, K. W. D. Ledingham, H. Genz, M. Mutterer, and R. L. Intemann, Orbital electron capture by the nucleus, *Rev. Mod. Phys.* **49**, 77 (1977).
- [12] P. Sarriguren, Electron-capture decay in isotopic transfermium chains from self-consistent calculations, *J. Phys. G: Nucl. Part. Phys.* **47**, 125107 (2020).
- [13] M. I. Eides, H. Grotch, and V. A. Shelyuto, Theory of light hydrogenlike atoms, *Physics Reports* **342**, 63 (2001).
- [14] T. Beier, H. Häffner, N. Hermanspahn, S. G. Karshenboim, H.-J. Kluge, W. Quint, S. Stahl, J. Verdú,

- and G. Werth, New determination of the electron's mass, *Phys. Rev. Lett.* **88**, 011603 (2001).
- [15] S. Sturm, F. Köhler, J. Zatorski, A. Wagner, Z. Harman, G. Werth, W. Quint, C. Keitel, and K. Blaum, High-precision measurement of the atomic mass of the electron, *Nature* **506**, 467 (2014).
- [16] N. S. Oreshkina, S. M. Cavaletto, N. Michel, Z. Harman, and C. H. Keitel, Hyperfine splitting in simple ions for the search of the variation of fundamental constants, *Phys. Rev. A* **96**, 030501(R) (2017).
- [17] A. V. Volotka and G. Plunien, Nuclear polarization study: New frontiers for tests of QED in heavy highly charged ions, *Phys. Rev. Lett.* **113**, 023002 (2014).
- [18] P. Indelicato, QED tests with highly charged ions, *J. Phys. B: At. Mol. Opt. Phys.* **52**, 232001 (2019).
- [19] K. Blaum, S. Eliseev, and S. Sturm, Perspectives on testing fundamental physics with highly charged ions in penning traps, *Quantum Sci. Technol.* **6**, 014002 (2020).
- [20] N. Paul, G. Bian, T. Azuma, S. Okada, and P. Indelicato, Testing quantum electrodynamics with exotic atoms, *Phys. Rev. Lett.* **126**, 173001 (2021).
- [21] T. Sailer, V. Debierre, Z. Harman, F. Heiße, C. König, J. Morgner, B. Tu, A. V. Volotka, C. H. Keitel, K. Blaum, and S. Sturm, Measurement of the bound-electron g-factor difference in coupled ions, *Nature* **606**, 479 (2022).
- [22] F. A. Parpia and W. R. Johnson, Radiative decay rates of metastable one-electron atoms, *Phys. Rev. A* **26**, 1142 (1982).
- [23] R. Popov and A. Maiorova, Relativistic calculations of one-photon transition probabilities in hydrogen-like ions, *Opt. Spectrosc.* **122**, 366 (2017).
- [24] J. Sommerfeldt, R. A. Müller, A. V. Volotka, S. Fritzsche, and A. Surzhykov, Vacuum polarization and finite-nuclear-size effects in the two-photon decay of hydrogenlike ions, *Phys. Rev. A* **102**, 042811 (2020).
- [25] A. Michels, J. De Boer, and A. Bijl, Remarks concerning molecular interaction and their influence on the polarisability, *Physica* **4**, 981 (1937).
- [26] E. Ley-Koo and S. Rubinstein, The hydrogen atom within spherical boxes with penetrable walls, *J. Chem. Phys.* **71**, 351 (1979).
- [27] M. N. Guimarães and F. V. Prudente, A study of the confined hydrogen atom using the finite element method, *J. Phys. B: At. Mol. Opt. Phys.* **38**, 2811 (2005).
- [28] R. Cabrera-Trujillo and S. A. Cruz, Confinement approach to pressure effects on the dipole and the generalized oscillator strength of atomic hydrogen, *Phys. Rev. A* **87**, 012502 (2013).
- [29] S. Goldman and C. Joslin, Spectroscopic properties of an isotropically compressed hydrogen atom,

- J. Phys. Chem. **96**, 6021 (1992).
- [30] C. Laughlin, On the dipole polarizability of a hydrogen-like atom confined in an impenetrable spherical box, *J. Phys. B: At. Mol. Opt. Phys.* **37**, 4085 (2004).
- [31] H. Montgomery and K. Sen, Dipole polarizabilities for a hydrogen atom confined in a penetrable sphere, *Phys. Lett. A* **376**, 1992 (2012).
- [32] J. A. Ludlow and T.-G. Lee, Investigating the static dipole polarizability of noble-gas atoms confined in impenetrable spheres and shells, *Phys. Rev. A* **91**, 032507 (2015).
- [33] N. Aquino, R. Rojas, and H. Montgomery, The energy correction due to a finite size nucleus of the hydrogen atom confined in a penetrable spherical cavity, *Rev. Mex. Fis.* **64**, 399 (2018).
- [34] K. Takahashi and K. Yokoi, Nuclear  $\beta$ -decays of highly ionized heavy atoms in stellar interiors, *Nucl. Phys. A* **404**, 578 (1983).
- [35] W. R. Phillips, I. Ahmad, D. W. Banes, B. G. Glagola, W. Henning, W. Kutschera, K. E. Rehm, J. P. Schiffer, and T. F. Wang, Charge-state dependence of nuclear lifetimes, *Phys. Rev. Lett.* **62**, 1025 (1989).
- [36] L. M. Folan and V. I. Tsifrinovich, Effects of the hyperfine interaction on orbital electron capture, *Phys. Rev. Lett.* **74**, 499 (1995).
- [37] Y. A. Litvinov, F. Bosch, H. Geissel, J. Kurcewicz, Z. Patyk, N. Winckler, L. Batist, K. Beckert, D. Boutin, C. Brandau, L. Chen, C. Dimopoulou, B. Fabian, T. Faestermann, A. Fragner, L. Grigorenko, E. Haettner, S. Hess, P. Kienle, R. Knöbel, C. Kozhuharov, S. A. Litvinov, L. Maier, M. Mazzocco, F. Montes, G. Münzenberg, A. Musumarra, C. Nociforo, F. Nolden, M. Pfützner, W. R. Plaß, A. Prochazka, R. Reda, R. Reuschl, C. Scheidenberger, M. Steck, T. Stöhlker, S. Torilov, M. Trassinelli, B. Sun, H. Weick, and M. Winkler, Measurement of the  $\beta^+$  and orbital electron-capture decay rates in fully ionized, hydrogenlike, and heliumlike  $^{140}\text{Pr}$  ions, *Phys. Rev. Lett.* **99**, 262501 (2007).
- [38] Z. Patyk, J. Kurcewicz, F. Bosch, H. Geissel, Y. A. Litvinov, and M. Pfützner, Orbital electron capture decay of hydrogen- and helium-like ions, *Phys. Rev. C* **77**, 014306 (2008).
- [39] A. N. Ivanov, M. Faber, R. Reda, and P. Kienle, Weak decays of H-like  $^{140}\text{Pr}^{58+}$  and He-like  $^{140}\text{Pr}^{57+}$  ions, *Phys. Rev. C* **78**, 025503 (2008).
- [40] N. Winckler, H. Geissel, Y. Litvinov, K. Beckert, F. Bosch, D. Boutin, C. Brandau, L. Chen, C. Dimopoulou, H. Essel, B. Fabian, T. Faestermann, A. Fragner, E. Haettner, S. Hess, P. Kienle, R. Knöbel, C. Kozhuharov, S. Litvinov, M. Mazzocco, F. Montes, G. Münzenberg, C. Nociforo, F. Nolden,

- Z. Patyk, W. Plaß, A. Prochazka, R. Reda, R. Reuschl, C. Scheidenberger, M. Steck, T. Stöhlker, S. Torilov, M. Trassinelli, B. Sun, H. Weick, and M. Winkler, Orbital electron capture decay of hydrogen- and helium-like  $^{142}\text{Pm}$  ions, *Phys. Lett. B* **679**, 36 (2009).
- [41] K. Siegień-Iwaniuk, N. Winckler, F. Bosch, H. Geissel, Y. A. Litvinov, and Z. Patyk, Orbital electron capture of hydrogen- and helium-like ions, *Phys. Rev. C* **84**, 014301 (2011).
- [42] F. Bosch, D. R. Atanasov, C. Brandau, I. Dillmann, C. Dimopoulou, T. Faestermann, H. Geissel, S. Hagmann, P.-M. Hillenbrand, P. Kienle, R. Knöbel, C. Kozhuharov, J. Kurcewicz, M. Lestinsky, S. A. Litvinov, Y. A. Litvinov, X. Ma, F. Nolden, T. Ohtsubo, Z. Patyk, R. Reuschl, M. S. Sanjari, C. Scheidenberger, D. Shubina, U. Spillmann, M. Steck, T. Stöhlker, B. Sun, M. Trassinelli, S. Trotsenko, X. L. Tu, H. Weick, N. Winckler, M. Winkler, D. F. A. Winters, T. Yamaguchi, and X. L. Yan, Beta decay of highly charged ions, *Phys. Scr.* **2013**, 014025 (2013).
- [43] F. Ozturk, B. Akkus, D. Atanasov, H. Beyer, F. Bosch, D. Boutin, C. Brandau, P. Bühler, R. Cakirli, R. Chen, W. Chen, X. Chen, I. Dillmann, C. Dimopoulou, W. Enders, H. Essel, T. Faestermann, O. Forstner, B. Gao, H. Geissel, R. Gernhäuser, R. Grisenti, A. Gumberidze, S. Hagmann, T. Heftrich, M. Heil, M. Herdrich, P.-M. Hillenbrand, T. Izumikawa, P. Kienle, C. Klaushofer, C. Kleffner, C. Kozhuharov, R. Knöbel, O. Kovalenko, S. Kreim, T. Kühl, C. Lederer-Woods, M. Lestinsky, S. Litvinov, Y. Litvinov, Z. Liu, X. Ma, L. Maier, B. Mei, H. Miura, I. Mukha, A. Najafi, D. Nagae, T. Nishimura, C. Nociforo, F. Nolden, T. Ohtsubo, Y. Oktem, S. Omika, A. Ozawa, N. Petridis, J. Piotrowski, R. Reifarh, J. Rossbach, R. Sánchez, M. Sanjari, C. Scheidenberger, R. Sidhu, H. Simon, U. Spillmann, M. Steck, T. Stöhlker, B. Sun, L. Susam, F. Suzaki, T. Suzuki, S. Torilov, C. Trageser, M. Trassinelli, S. Trotsenko, X. Tu, P. Walker, M. Wang, G. Weber, H. Weick, N. Winckler, D. Winters, P. Woods, T. Yamaguchi, X. Xu, X. Yan, J. Yang, Y. Yuan, Y. Zhang, and X. Zhou, New test of modulated electron capture decay of hydrogen-like  $^{142}\text{Pm}$  ions: Precision measurement of purely exponential decay, *Phys. Lett. B* **797**, 134800 (2019).
- [44] W. K. Hensley, W. A. Bassett, and J. R. Huizenga, Pressure dependence of the radioactive decay constant of beryllium-7, *Science* **181**, 1164 (1973).
- [45] L. gun Liu and C.-A. Huh, Effect of pressure on the decay rate of  $^7\text{Be}$ , *Earth Plan. Sci. Lett.* **180**, 163 (2000).
- [46] K. K. Lee and G. Steinle-Neumann, Ab-initio study of the effects of pressure and chemistry on the electron-capture radioactive decay constants of  $^7\text{Be}$ ,  $^{22}\text{Na}$  and  $^{40}\text{K}$ , *Earth Plan. Sci. Lett.* **267**, 628 (2008).

- [47] A. Ray, P. Das, A. Sikdar, S. Pathak, N. Aquino, M. Lozano-Espinosa, and A. Artemyev, Electron capture nuclear decay rate under compression in a confined environment, *Eur. Phys. J. D* **75**, 140 (2021).
- [48] T. Ohtsuki, H. Yuki, M. Muto, J. Kasagi, and K. Ohno, Enhanced electron-capture decay rate of  ${}^7\text{Be}$  encapsulated in  $\text{C}_{60}$  cages, *Phys. Rev. Lett.* **93**, 112501 (2004).
- [49] T. Ohtsuki, K. Ohno, T. Morisato, T. Mitsugashira, K. Hirose, H. Yuki, and J. Kasagi, Radioactive decay speedup at  $t = 5$  K: Electron-capture decay rate of  ${}^7\text{Be}$  encapsulated in  $\text{C}_{60}$ , *Phys. Rev. Lett.* **98**, 252501 (2007).
- [50] T. Morisato, K. Ohno, T. Ohtsuki, K. Hirose, M. Sluiter, and Y. Kawazoe, Electron-capture decay rate of  ${}^7\text{Be}@_{\text{C}_{60}}$  by first-principles calculations based on density functional theory, *Phys. Rev. B* **78**, 125416 (2008).
- [51] R. Kuwahara, K. Ohno, and T. Ohtsuki, Electron-capture decay rate of  ${}^7\text{Be}$  in cluster and crystal forms of beryllium: A first-principles study, *Phys. Rev. C* **109**, 024609 (2024).
- [52] T. S. Shang, H. H. Xie, J. Li, and H. Liang, Global prediction of nuclear charge density distributions using a deep neural network, *Phys. Rev. C* **110**, 014308 (2024).
- [53] T. S. Shang, J. Li, and Z. M. Niu, Prediction of nuclear charge density distribution with feedback neural network, *Nucl. Sci. Tech.* **33**, 153 (2022).
- [54] Y. D. Wang, T. S. Shang, H. H. Xie, P. X. Du, J. Li, and H. Z. Liang, Predictions of charge density distributions for nuclei with  $Z \geq 8$ , *Nucl. Sci. Tech.* **37**, 93 (2026).
- [55] L. G. Jiao, Y. Y. He, A. Liu, Y. Z. Zhang, and Y. K. Ho, Development of the kinetically and atomically balanced generalized pseudospectral method, *Phys. Rev. A* **104**, 022801 (2021).
- [56] S.-I. Chu and D. A. Telnov, Beyond the floquet theorem: generalized floquet formalisms and quasienergy methods for atomic and molecular multiphoton processes in intense laser fields, *Phys. Rep.* **390**, 1 (2004).
- [57] H. H. Xie, L. G. Jiao, A. Liu, and Y. K. Ho, High-precision calculation of relativistic corrections for hydrogen-like atoms with screened coulomb potentials, *Int. J. Quantum Chem.* **121**, e26653 (2021).
- [58] L. G. Jiao, H. H. Xie, A. Liu, H. E. Montgomery, and Y. K. Ho, Critical screening parameters and critical behaviors of one-electron systems with screened coulomb potentials, *J. Phys. B: At. Mol. Opt. Phys.* **54**, 175002 (2021).
- [59] L. Zhu, Y. Y. He, L. G. Jiao, Y. C. Wang, and Y. K. Ho, Revisiting the generalized pseudospectral method: Radial expectation values, fine structure, and hyperfine splitting of confined atom, *Int J Quantum Chem.* **120**, e26245 (2020).

- [60] C. Wang, T. Naito, J. Li, and H. Liang, A deep neural network approach to solve the dirac equation, *Eur. Phys. J. A* **61**, 162 (2025).
- [61] C. Wang, T. Naito, J. Li, and H. Liang, A neural network approach for two-body systems with spin and isospin degrees (2024), [arXiv:2403.16819](https://arxiv.org/abs/2403.16819).
- [62] E. Wigner and H. B. Huntington, On the possibility of a metallic modification of hydrogen, *The Journal of Chemical Physics* **3**, 764 (1935).